

# Effects of Loadings on Friction and Wear Behaviors of Cathodic Arc Ion Plating AlTiN Coating at High Temperature

Kong Dejun<sup>a,b</sup>, Guo Haoyuan<sup>a</sup>, and Wang Wenchang<sup>a</sup>

<sup>a</sup>College of Mechanical Engineering, Changzhou University, Changzhou, PR China; <sup>b</sup>Jiangsu Key Laboratory of Materials Surface Science and Technology, Changzhou University, Changzhou, PR China

## ABSTRACT

A layer of AlTiN coating was deposited on YT14 cutting tool by cathodic arc ion plating (CAIP) and the coefficients of friction (COFs) of the AlTiN coating under different loads at a temperature of 800°C were investigated with a high-temperature wear tester. The wear morphologies, chemical elements, and phases of the coating after wear were analyzed with scanning electron microscopy (SEM), energy-dispersive spectrometry (EDS), and X-ray diffraction (XRD), respectively, and the contours of wear tracks were investigated with a comprehensive measurement tester for material surface performance. The effects of loads on COFs and wear resistance of the AlTiN coating were analyzed, and the wear mechanism of the AlTiN coating at high temperature is discussed. The results show that the mixed oxides of Al<sub>2</sub>O<sub>3</sub> and TiO<sub>2</sub> are produced under high temperature to improve the lubrication performance and wear resistance of the AlTiN coating. The average COFs of the coating under loads of 5, 7, and 9 N are 0.6495, 0.5897, and 0.3898, respectively. The COFs of the coating decrease with increasing load; as a result, the AlTiN coating is suitable for heavy loads at high temperature. The friction and wear mechanisms of the AlTiN coating are primarily composed of oxidation wear and abrasive wear, accompanied by fatigue wear and adhesive wear.

## ARTICLE HISTORY

Received 25 May 2015  
Accepted 10 September 2015

## KEY WORDS

AlTiN coating; high-temperature friction and wear; coefficient of friction (COF); wear mechanism

## Introduction

With the development of coating technologies and higher requirements for mechanical properties, the coating ability of cutting tools with wear resistance and oxidation resistance at high temperatures have been investigated (Zhang, et al. (1)). Due to brittleness, low hardness and oxidation at high temperature, the traditional TiN coating cannot satisfy the above requirements (Kong and Fu (2); Tian, et al. (3); Chang and Wang (4)). Al atoms are introduced into TiN to form an AlTiN coating, which changes the coating microstructures and crystallographic orientation. The hardness, wear resistance, and oxidation resistance of the AlTiN coating at high temperatures are higher than those of the TiN coating, and the oxidation temperature can reach 800°C (Jilek, et al. (5); Halil, et al. (6); Kong and Guo (7); Wang, et al. (8)). The dense mixed oxides of Al<sub>2</sub>O<sub>3</sub> and TiO<sub>2</sub> are produced on the AlTiN surface at high temperatures, in which the TiO<sub>2</sub> plays the role of lubrication and the Al<sub>2</sub>O<sub>3</sub> plays the role of wear resistance and oxidation resistance (Kong and Guo (9); Xie, et al. (10); Radhika, et al. (11)); therefore, the AlTiN coating is suitable for surface modification of cutting tools at high speed. Many researchers have investigated the AlTiN coating applications in China and abroad, but few have reported on the friction and wear mechanisms of AlTiN coating at high temperatures, especially the wear characteristics under different loads (Kong and Fu (2); Radhika, et al. (11)). A layer of AlTiN coating was deposited on a YT14 cutting tool with cathodic arc ion plating

(CAIP) in this study, and the coefficients of friction (COFs) and wear morphologies of AlTiN coatings under loads of 5, 7, and 9 N were investigated at 800°C, which was the highest working temperature of the coating. The surface morphologies, phases, and plane scans of the AlTiN coating after high-temperature wear were analyzed with scanning electron microscopy (SEM), X-ray diffraction (XRD), and energy-dispersive spectrometry (EDS), respectively, which provided an experimental basis for investigating the friction and wear behaviors and wear mechanisms of the AlTiN coating at high temperatures.

## Experimental

The YT14 cutting tool was adopted as the substrate material with the chemical compositions as follows (mass, %): WC 78, TiC 14, Co 8. Before deposition, the samples were ground using 80-, 120-, 200-, 600-, 800-, 1,200-mesh sandpapers and metallographic sandpaper and polished on a polishing machine. Then the samples were cleaned in pure acetone using ultrasonic oscillation and rinsed in pure ethanol and dried before being deposited on a CAIP coating system. During deposition of the AlTiN coatings, industrial Ar and N<sub>2</sub> gases with purity of 99.99% were adopted as the working gases. The targets were composed of Al and Ti with purity of 99.9999%; see Fig. 1. The technological parameters of CAIP were as follows: bias power

**CONTACT** Kong Dejun  [kong-dejun@163.com](mailto:kong-dejun@163.com)

Color versions of one or more of the figures in the article can be found online at [www.tandfonline.com/utrb](http://www.tandfonline.com/utrb).

Review led by Gary Doll

© 2016 Society of Tribologists and Lubrication Engineers

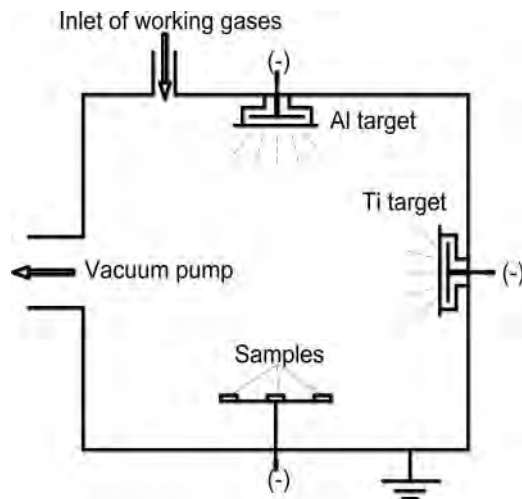


Figure 1. Sketch of cathodic arc ion-plated AlTiN coating.

of  $-100$  V, target current of 70 A, duty cycle (i.e., ratio of power time and power cycle of pulse signal) of 30%, gas pressure of 1.2 Pa, working temperature of  $500^{\circ}\text{C}$ , and deposition time of 120 min. After pretreatment, the surface-interface morphologies of the coating were analyzed with a field-emission SEM, and the surface roughness of the AlTiN coating was measured with an atomic force microscope, with a sampling range of  $90,000\text{ nm} \times 90,000\text{ nm}$ . High-temperature friction and wear tests of the AlTiN coatings were conducted on a high-temperature wear tester as follows: friction mode, sliding; friction pair, ceramic ( $\text{Si}_3\text{N}_4$ ) ball with a diameter of 6 mm; load, 5, 7, and 9 N; rotation speed, 500 rpm; gyration radius, 5 mm; working temperature,  $800^{\circ}\text{C}$ . The worn contours of the AlTiN coating were investigated on a comprehensive measurement tester for material surface performance. The wear morphologies, plane scans, and phases of the AlTiN coatings after high-temperature wear were observed with a configured SEM, configured EDS, and XRD, respectively.

## Analysis of results

### Surface morphologies and EDS analysis

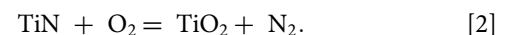
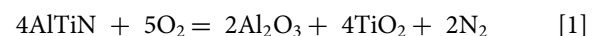
The surface morphology of the AlTiN coating showed a unique blue-gray color with roughness and a few different sized white bright droplets and black holes, as shown in

Fig. 2a. There were three chemical elements, Al, Ti, and N, in the AlTiN coating, with mass fractions (mass, %) as follows: Al 46.12 Ti 30.34, N 23.54. The content of Al was higher than that of Ti, which was two times greater than the N content. This indicates that the high Al content of the AlTiN coating had been deposited successfully, as shown in Fig. 2b. Figure 2c shows the interfacial morphology of the AlTiN coating with a thickness of about  $1.75\text{ }\mu\text{m}$ . The coating had a uniform structure, and the interface of the coating and substrate was evident.

### XRD analysis

The XRD analysis results of the AlTiN coating at normal temperature are shown in Fig. 3a, in which the diffraction peaks of AlTiN, TiN, and the substrate were detected. This was because the thickness of AlTiN coating was only  $1.75\text{ }\mu\text{m}$ , so X-rays can penetrate the coating and therefore the strong diffraction peak of the substrate was detected. The TiN coating was a B1-NaCl type face-centered cubic structure. Al atoms were introduced into the TiN coating to provide the high Al content of the AlTiN coating. Thus, the lattice coefficient changed and the gap between the atoms was reduced, and the oxidation resistance of the AlTiN coating increased. At  $800^{\circ}\text{C}$ , the strong diffraction peaks of  $\text{Al}_2\text{O}_3$  and  $\text{TiO}_2$  were detected on the coating surface, which showed that the oxidation reaction occurred at that temperature. In addition, mixed oxide films were formed; the surface element contents were enriched by Al and deficient in Ti, whereas the inner layer were enriched in Ti and deficient in Al, which played a role in lubrication and antifriction.

At  $800^{\circ}\text{C}$ , the reactions of the AlTiN coating were produced as follows:



According to the thermodynamic handbook, the Gibbs free energy of Ti and 1 mol  $\text{O}_2$  reacted to produce  $\text{TiO}_2$  as follows:

$$\Delta G_{\text{TiO}_2}^{\theta} = -749.4\text{ kJ}. \quad [3]$$

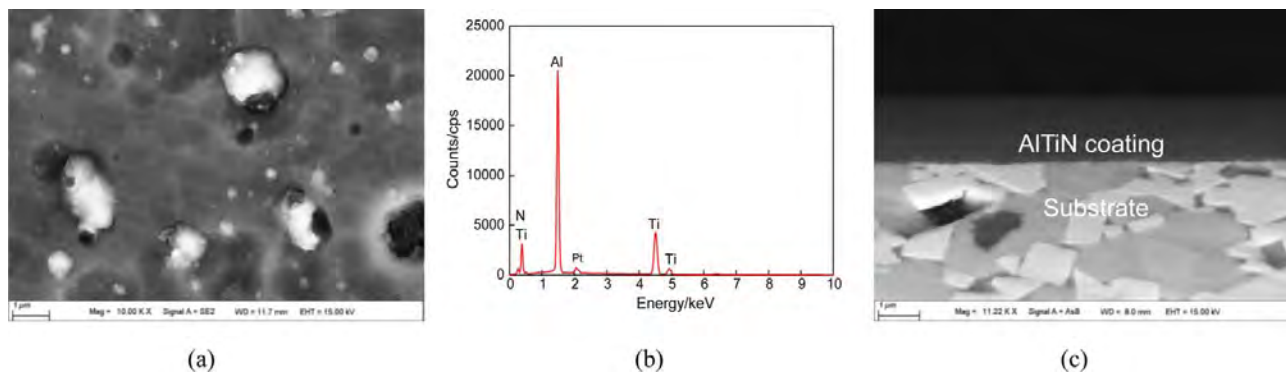


Figure 2. Surface-interface morphologies and EDS analysis of the AlTiN coating: (a) surface, (b) EDS analysis, and (c) interface.

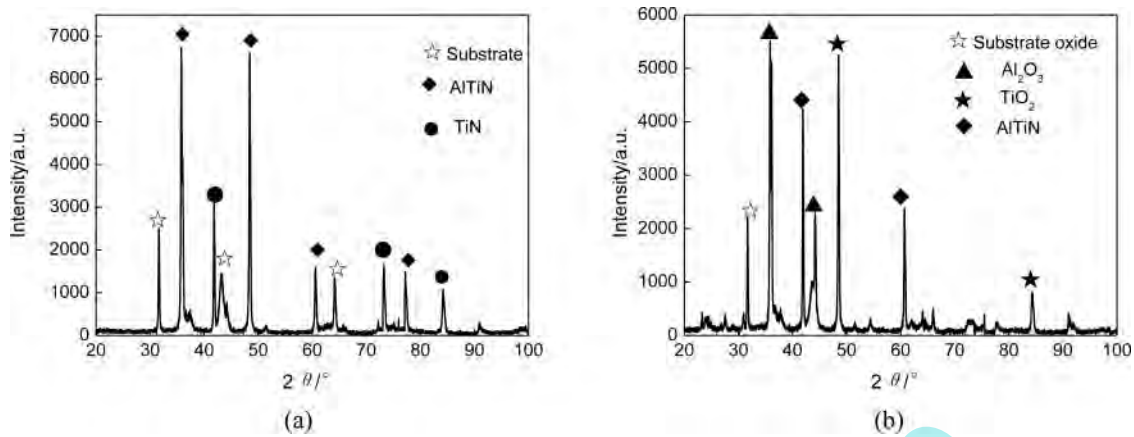


Figure 3. XRD analysis of AlTiN coatings at: (a) normal temperature and (b) 800°C.

The Gibbs free energy of  $\text{Al}_2\text{O}_3$  by the reaction of Al and 1.5 mol  $\text{O}_2$  is as follows:

$$\Delta G_{\text{Al}_2\text{O}_3}^\theta = -903.5 \text{ kJ}. \quad [4]$$

Thus,

$$|\Delta G_{\text{Al}_2\text{O}_3}^\theta| > |\Delta G_{\text{TiO}_2}^\theta|. \quad [5]$$

According to Eq. [5], the absolute value of the  $\text{Al}_2\text{O}_3$  Gibbs free energy was higher than that of the  $\text{TiO}_2$ , which indicated that the high-temperature thermodynamic driving force generating  $\text{Al}_2\text{O}_3$  was greater than that generating  $\text{TiO}_2$ . The Al atoms had quite strong affinity with the O atoms and took priority over the generation of  $\text{TiO}_2$  (Yucel (13)). The  $\text{Al}_2\text{O}_3$  film was a continuous, dense, and stable structure, which hindered the O atoms from further diffusing into the internal coating and the Ti atoms from diffusing to the coating surface. At 800°C, the diffraction peaks of the substrate oxides were also detected, showing that the O atoms reacted with the substrate directly to generate oxides. Moreover, a part of the coating surface had been severely damaged and the channel between the

oxygen in the air, and the substrate was punctured. Finally, the isolation role of the oxide films between the O elements and substrate became weak. At the same time, the diffraction peak of the AlTiN phase was still obvious, showing that the coatings were not completely oxidized and exfoliated, which still played a protective role and prevented the coating from being further oxidized, as shown in Fig. 3b.

### Surface roughness

Figure 4a shows the atomic force microscope image of the YT14 cutting tool after polishing. The surface roughness values were calculated as follows:  $S_a$  (average roughness) = 0.108 nm,  $S_q$  (mean square root) = 0.006 nm,  $S_{sk}$  (surface skewness) = -11.1,  $S_{ku}$  (surface kurtosis) = 392,  $S_y$  (peak-peak height) = 1 nm, and  $S_z$  (10-point height) = 0.935 nm. Some rough pits existed on the AlTiN coating surface, as shown in Fig. 4b. The roughness of the surface was lower and there were only a few topographies with similar macroparticles, which increased the surface roughness. The surface roughness values were calculated as follows:  $S_a = 0.108 \text{ nm}$ ,  $S_q = 0.142 \mu\text{m}$ ,  $S_{sk} = 0.216$ ,  $S_{ku} = 3.4$ ,  $S_y = 0.992 \text{ nm}$ , and  $S_z = 0.992 \text{ nm}$ , as shown in

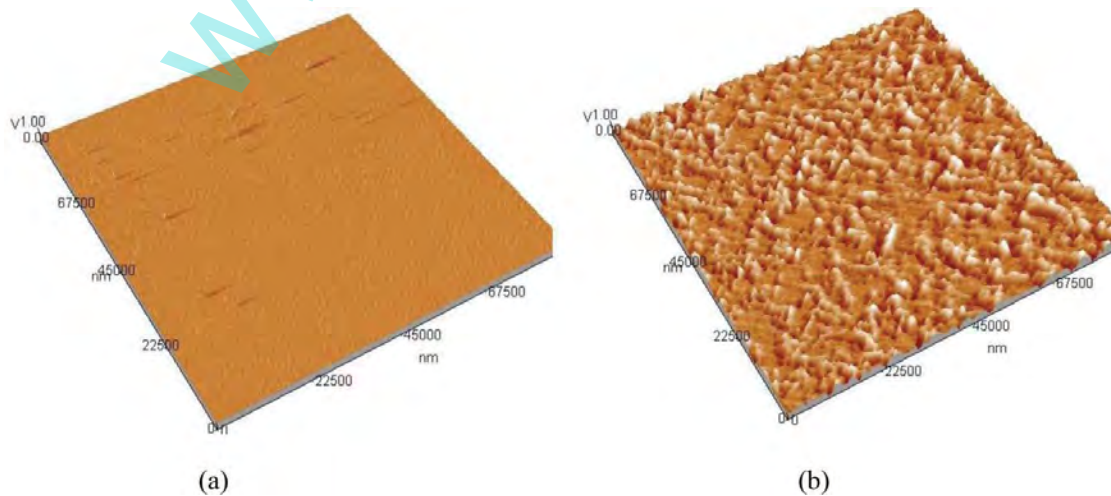


Figure 4. Surface roughness of the (a) substrate and (b) AlTiN coating.

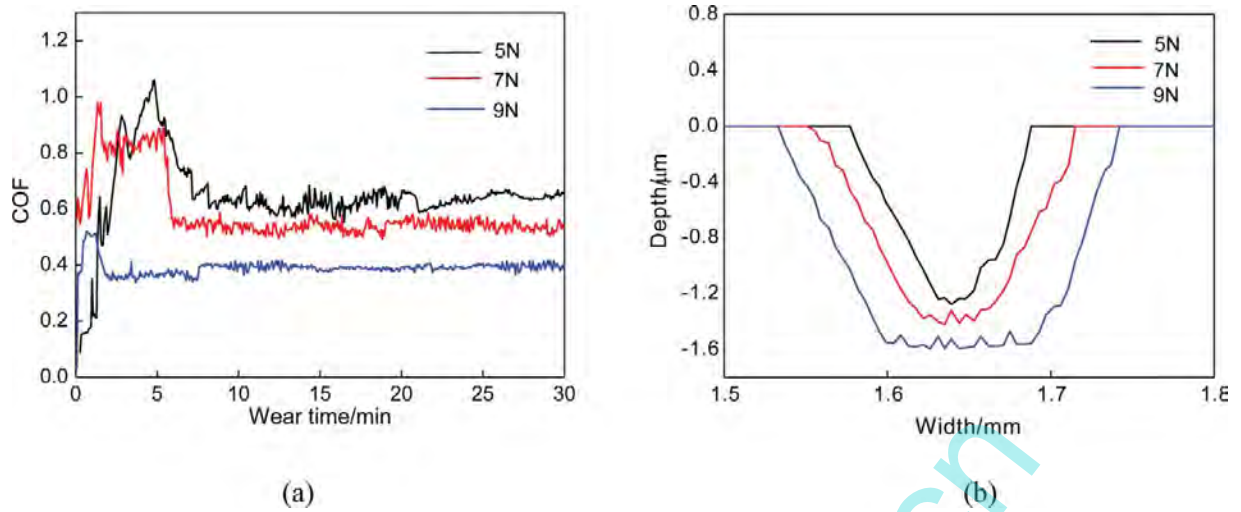


Figure 5. (a) COFs vs. wear time and (b) contours of the wear track.

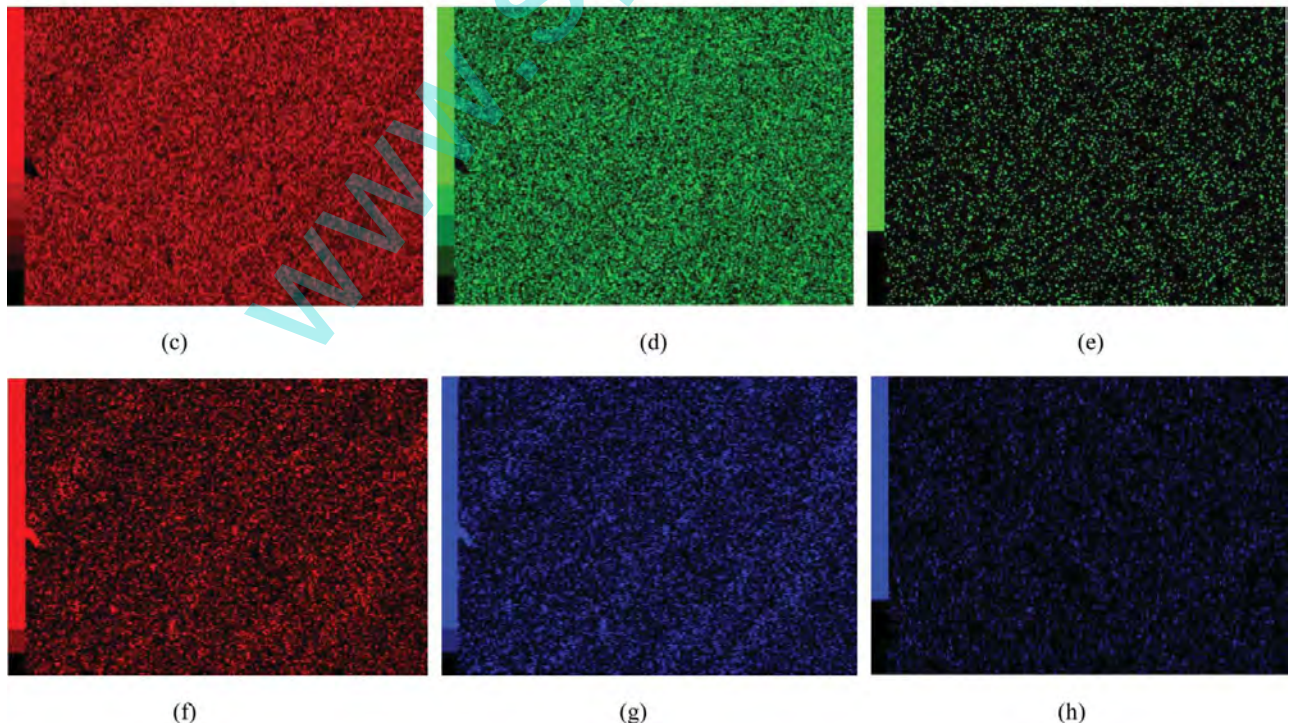
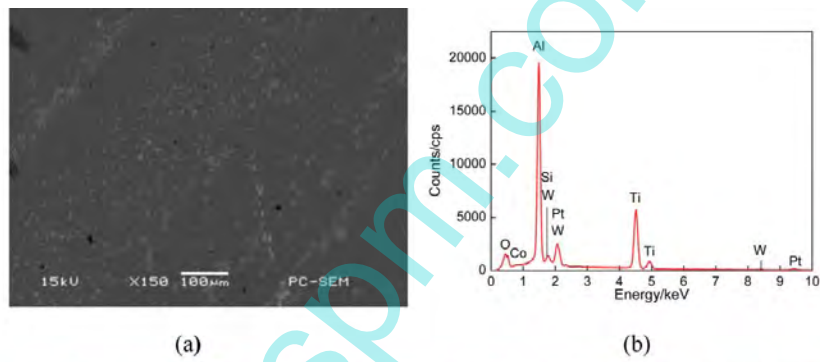


Figure 6. Plane scans of AlTiN coating surface under a load of 5 N (a) scanned position; (b) result of plane scan; (c) Al content; (d) Ti content; (e) O content; (f) Si content; (g) W content; and (h) Co content.

**Fig. 4b.** From the above analyses, it can be seen that the surface roughness of the coating increased after CAIP, which had a certain influence on friction and wear.

### COFs and wear track contour

The relationship between the COFs of the AlTiN coating and wear time under loads of 5, 7, and 9 N at 800°C is shown in Fig. 5a. The average COF of the AlTiN coating was 0.6495 under a load of 5 N for 30 min, and that under a load of 7 N was 0.5897, which was reduced by 9.21% compared to that under a load of 5 N. The average COF of the AlTiN coating under a load of 9 N was 0.3898, reduced by 39.98 and 33.90% compared with to under loads of 5 and 7 N, respectively. Therefore, the COFs of the AlTiN coating reduced with increasing load at 800°C. Under a load of 5 N, the average COF of the stable stage was 0.6301, compared to 0.5399 under a load of 7 N and 0.3874 under a load of 9 N. The running-in stage increased and the stable stage began later. Moreover, the COF of the

stable stage fluctuated gently. This was because the normal stress and the contact stress of the friction pair surface increased with increasing load. The surface roughness of the coating was rubbed out and the pits were filled quickly, which made the coating enter the stable stage faster under heavy loads. In addition, the shear stress of the friction pairs increased under heavy loads, and the temperature of the friction interface rose faster. The mixed oxide films of Al<sub>2</sub>O<sub>3</sub> and TiO<sub>2</sub> were produced, of which the TiO<sub>2</sub> played a role in lubrication, changing the interfacial contact area and bearing behavior, which made the COFs of the stable stage smoother. The contour curves of wear tracks at different loads are shown in Fig. 5b. The maximum wear track depths under loads of 5, 7, and 9 N were 1.28, 1.42, and 1.59 μm, respectively, and the corresponding maximum wear track widths were 111, 164, and 209 μm, respectively. It can be seen that the depth and width of the wear track decreased with increasing load, showing that the wear track depth of the coating deepened and the wear track widened at high temperature, but the coating did not wear out.

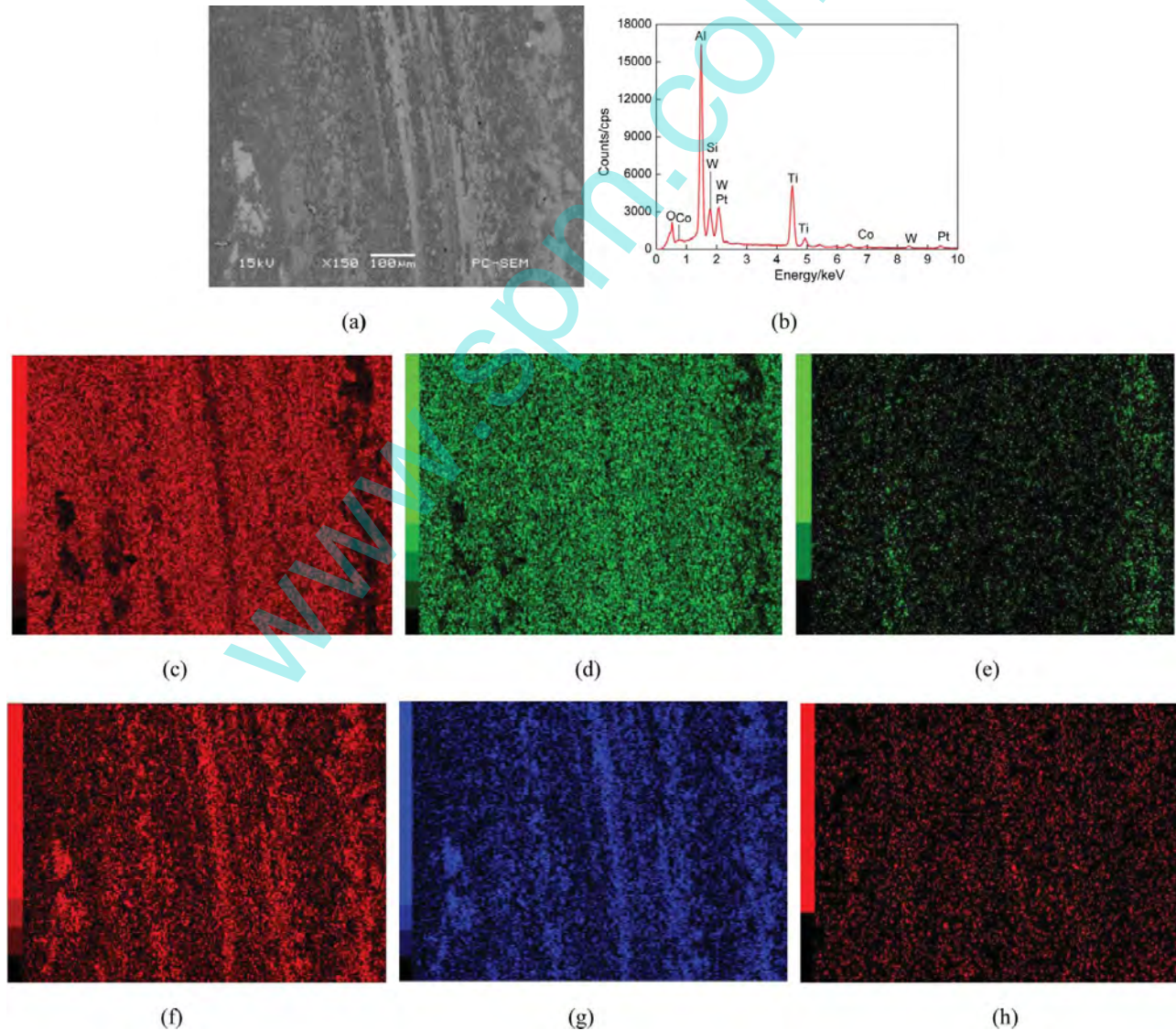


**Figure 7.** Plane scans of AlTiN coating surface under a load of 7 N: (a) scanned position; (b) result of plane scan; (c) Al content; (d) Ti content; (e) O content; (f) Si content; (g) W content; and (h) Co content.

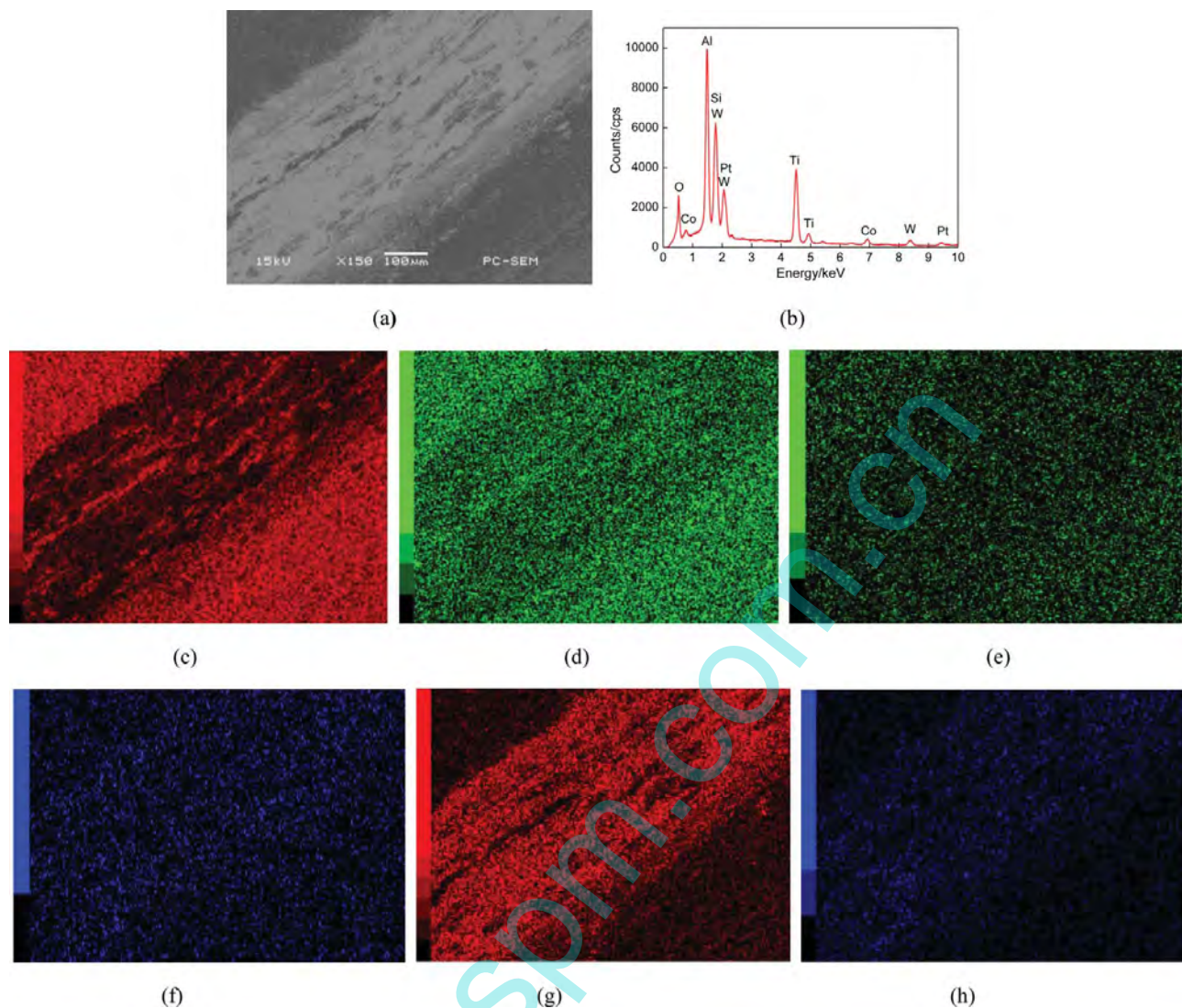


**Figure 8.** Plane scans of AlTiN coating surface under a load of 9 N: (a) scanned position; (b) result of plane scan; (c) Al content; (d) Ti content; (e) O content; (f) Si content; (g) W content; and (h) Co content.

Because the dense and stable  $\text{Al}_2\text{O}_3$  phase was produced, the excellent oxidation resistance ability of AlTiN coating at high temperature was improved to a certain extent. Although the  $\text{Al}_2\text{O}_3$  played a role in wear resistance and oxidation resistance, the cyclic shear stress increased, accelerating initiation and propagation of cracks and the normal load increased. In addition, the high strength of  $\text{Al}_2\text{O}_3$  and the hard particles cut the coating under high stress, which accelerated wear of the coating. According to the above analyses, the AlTiN coating was suitable for dry wear under heavy loads and provided a protective effect on the substrate. Therefore, the AlTiN coating showed good performance for oxidation wear resistance at high temperature.

#### Plane scans of the wear track

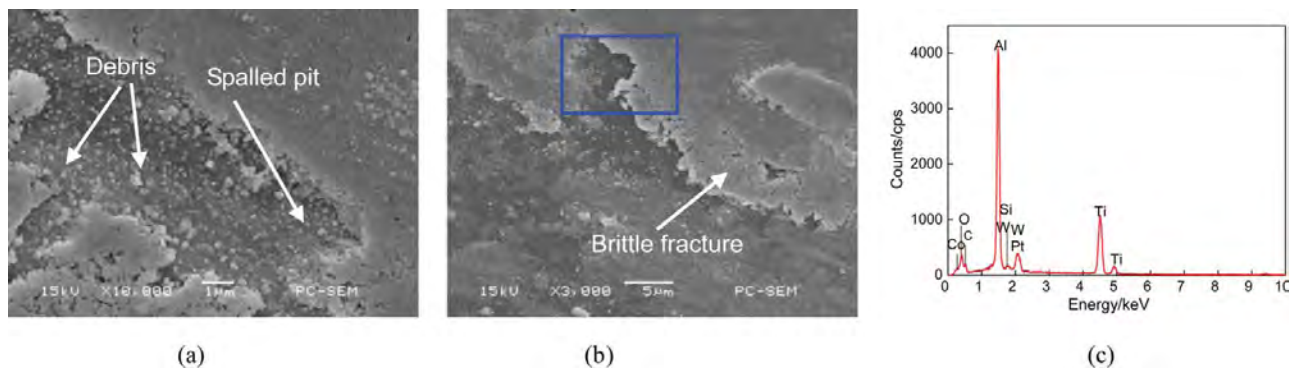
##### Plane scans of the wear track at 5 N

Figure 6a shows the plane scanned position of the wear track under a load of 5 N. The plane scan results of the wear track are shown in Fig. 6b. The mass fractions (mass, %) of the wear track were as follows: Al 28.36, Ti 41.42, O 12.33, Si 0.82, W

16.41, Co 0.65; the atomic fractions (at, %) were as follows: Al 37.33, Ti 30.67, O 27.39, Si 1.05, W 3.17, Co 0.39. Many Al and Ti atoms still existed on the wear track and were distributed uniformly, and there was no stacked enrichment phenomenon, as shown in Figs. 6c and 6d. The N element was not detected, which was because the N atoms of the coating were fully released at high temperature. The content of O element was higher on the wear track, and there were a small number of Si atoms, which showed that friction oxidation of the AlTiN coating occurred during wear, and the AlTiN coating particles with high hardness and the  $\text{Si}_3\text{N}_4$  ball produced a certain amount of wear. Moreover, exfoliations with the chips were oxidized on the wear track, as shown in Figs. 6e and 6f. A small number of W and C atoms were detected on the wear track, which came from the substrate and were distributed uniformly on the wear track, as shown in Figs. 6g and 6h.

##### Plane scans of the wear track at 7 N

The plane scanned position of the wear track under a load of 7 N is shown in Fig. 7a. The result of the plane scan is shown in Fig. 7b. The mass fractions (mass, %) of the wear track were



**Figure 9.** Wear morphologies of AlTiN coating under a load of 5 N and EDS analysis (a) high magnification; (b) low magnification; and (c) EDS analysis.

shown as follows: Al 28.16, Ti 42.08, O 12.42, Si 0.90, W 15.85, Co 0.6; the atomic fractions (at, %) were as follows: O 36.93, Al 31.04, Si 27.48, Ti 1.14, Co 3.05, W 0.36. Compared to that under a load of 5 N, the wear particles increased and aggravated wear of the coating. There were clear shedded tracks in the wear direction, and the edge of the wear track was heavily worn with evident black zones, which were the dim parts of Al and Ti elements. This was because the peeled hard coating particles ploughed the wear track surface, as shown in Figs. 7c and 7d. The plane scan of O element was brighter than that under a load of 5 N, showing that the AlTiN coating was further oxidized with increasing load, as shown in Fig. 7e. In addition, mixed oxide films of  $\text{Al}_2\text{O}_3$  and  $\text{TiO}_2$  were produced, which improved the wear properties of the coating. The plane scan of Si element was also brighter than that under a load of 5 N, which indicated that the lower hardness of the ceramic ball resulted in more severe wear with increasing load and transfer to the coating surface, as shown in Fig. 7f. The W and C contents of the wear track also increased correspondingly, because the substrate atoms were diffused under high temperature, as shown in Figs. 7g and 7h.

#### Plane scans of the wear track at 9 N

The plane scanned position of the wear track under a load of 9 N is shown in Fig. 8a. As can be seen, there were evident wear tracks and the coating was severely worn, with grinding cracks in the wear direction. The mass fractions (mass, %) of the wear track were as follows: Al 28.42, Ti 41.19, O 12.22, Si 1.04, W

2.53, Co 0.51; the atomic fractions (at, %) were as follows: O 37.45, Al 30.53, Ti 27.18, Co 3.21, W 0.31, as shown in Fig. 8b. A large part of the AlTiN coating wore out, and the Al atoms were reduced on the wear track, as shown in Fig. 8c. The plane scan of Ti element was not the same as that of the Al element on the wear track, appearing as a large area of bright black bands, because part of the Ti atoms came from the YT14 cutting tool, as shown in Fig. 8d. Moreover, a large number of O atoms were detected on the wear track with a uniform distribution, as shown in Fig. 8e. The O atoms came from the following sources:

1. Mixed oxide films of  $\text{Al}_2\text{O}_3$  and  $\text{TiO}_2$  were produced during wear, and the oxidation mechanism of the AlTiN coating was as follows: the Al atoms were diffused toward the coating surface faster than that of Ti atoms at high temperature, so they were enriched in Al and deficient in Ti, and oxide films were formed on the coating surface. On the contrary, the inside of the coating was enriched in Ti and deficient in Al. The Al atoms on the coating surface were combined with O atoms to form dense  $\text{Al}_2\text{O}_3$ , and a small number of O atoms reacted with Ti atoms through the  $\text{Al}_2\text{O}_3$  layer to form  $\text{TiO}_2$ . Ultimately, the  $\text{Al}_2\text{O}_3$  and  $\text{TiO}_2$  oxidation structure was produced (Chen, et al. (14)).
2. The Si atoms of the ball were transferred to the coating surface and gathered in the form of wear particles on the wear track. The Si content increased and was brightly colored, as shown in Fig. 8f. The W and C elements were

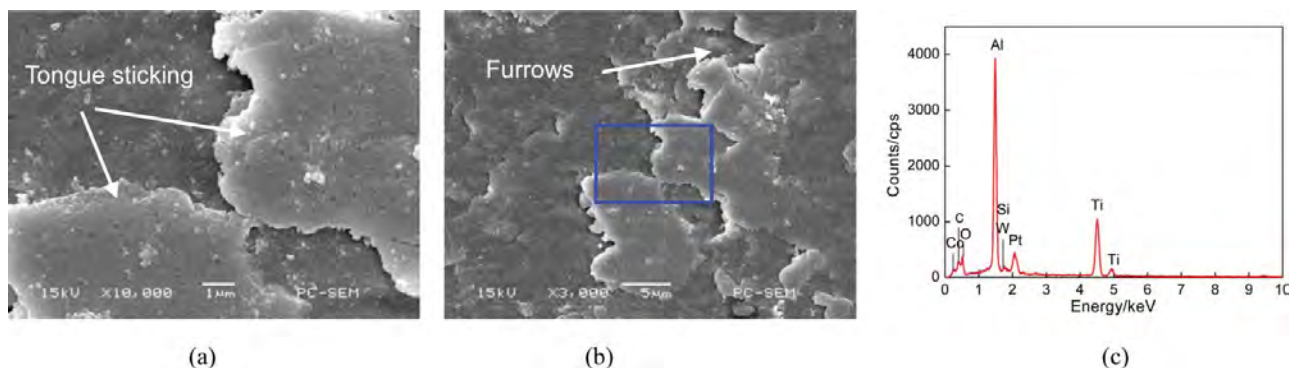


**Figure 10.** Wear morphologies of AlTiN coating under a load of 7 N and EDS analysis: (a) high magnification; (b) low magnification; and (c) EDS analysis.

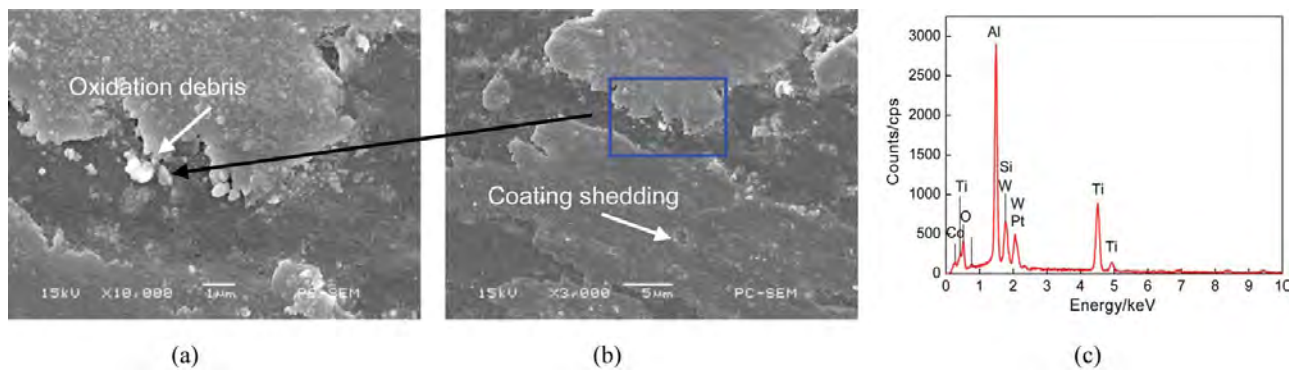


Figure 11. Wear morphologies of AlTiN coating under a load of 9 N and EDS analysis: (a) high magnification; (b) low magnification; and (c) EDS analysis.

distributed uniformly on the wear track, as shown in Figs. 8g and 8h.

### Wear mechanism

#### Wear morphologies and EDS analysis under a load of 5 N

The worn surface of the AlTiN coating was rough under a load of 5 N, with a lot of debris and pits. The shedded insets are shown in Fig. 9a. It can be seen that a lot of wear particles existed on the pits, which was because the debris was not discharged quickly, there was no accumulation, and brittle rupture of the coating occurred, as shown in Fig. 9b. This was because the oxide films had a certain brittleness and were easily crushed under a large circulating pressure. Thereby, the oxide films were flaked, appearing as a stripped layer. The EDS analysis result of the wear track in Fig. 9b is shown Fig. 9c. The mass fractions (mass, %) were as follows: Al 28.61, Ti 40.63, Si 0.93, O 12.52, W 16.09, C 0.70, Co 0.53; the atomic fractions (at, %) were as follows: Al 36.84, Ti 29.43, Si 1.15, O 27.21, W 3.04, C 2.02, Co 0.31. The Al, Ti, and O elements were the primary elements on the wear track. The N element was not detected, indicating that it was fully released after high-temperature oxidation. Mixed oxide films of  $\text{Al}_2\text{O}_3$  and  $\text{TiO}_2$  were generated, among which the shear strength of  $\text{TiO}_2$  was very low, playing a role in lubrication, and the dense stability of  $\text{Al}_2\text{O}_3$  played a role in oxidation resistance. Therefore, the wear mechanism of the AlTiN coating was primarily composed of oxidation at high temperature, and the W, C, and Co elements came from the chemical elements of the substrate.

#### Wear morphologies and EDS Analysis under a Load of 7 N

There were a large number of debris layers accumulated on the worn surface of the AlTiN coating under a load of 7 N. The debris was adhered to the coating surface with a tongue shape, as shown in Fig. 10a. This was because a compacted oxide layer was formed on the worn surface under the alternating pressure. In addition, the hard particles cut the coating, forming a furrowed topography, which presented an obvious abrasive wear mechanism (Soner and Şengül (15); Biksa, et al. (16)), as shown in Fig. 10b. Figure 10c shows the EDS analysis result for Fig. 10b; the mass fractions (mass, %) were as follows: Al 27.28, Ti 37.92, Si 1.10, O 14.98, W 17.39, C 0.75, Co 0.57; the atomic fractions (at, %) were as follows: Al 36.84, Ti 29.43, Si 1.15, O 27.21, W 3.04, C 2.02, Co 0.31. The fractions of Al and Ti atoms

were reduced, but the O atom fraction increased compared to that under a load of 5 N, showing that with increasing load, the wear mechanism was primarily oxidation wear. The emergence and rupture of oxidation film led to changes in the contents of Al, Ti, and O elements. The Si content increased because the hardness of  $\text{Si}_3\text{N}_4$  was lower than that of the AlTiN coating which was the covalent bond as the same as the coating. As the load increased, the grinding ball was adhered to the coating surface and oxidized, and the W, C, and Co elements came from the substrate.

#### Wear morphologies and EDS analysis under a load of 9 N

The wear track of the AlTiN coating was divided into a debris compaction zone and debris peeling zone under a load of 9 N. The coating was severely bruised and appeared plastic plow and furrowed in the wear direction, as shown in Figs. 11a and 11b, showing an abrasive wear mechanism. Figure 11c shows the EDS analysis result of the wear track in Fig. 11b. The mass fractions (mass, %) were as follows: Al 25.69, Ti 35.51, Si 1.29, O 17.41, W 18.68, C 0.80, Co 0.62; the atomic fractions (at, %) were as follows: Al 36.84, Ti 29.43, Si 1.15, O 27.21, W 3.04, C 2.02, Co 0.31. Compared to loads of 5 and 7 N, the contents of Al and Ti were decreased under a load of 9 N. However, the Ti elements did not decrease as significantly as the Al element, because the coating wore continuously with flaking and some elements of the substrate were detected under heavy load, which was proved by increasing of W and Co elements. The increasing O and Si elements showed that the oxidation wear was more violent and the grinding ball was adhered to the coating.

### Conclusions

1. The N element of the AlTiN coating is fully released at  $800^\circ\text{C}$ , and the mixed films of  $\text{Al}_2\text{O}_3$  and  $\text{TiO}_2$  are produced. The  $\text{Al}_2\text{O}_3$  plays a role in wear resistance and oxidation resistance, which improves the wear property of the coating, and the  $\text{TiO}_2$  plays a role in lubrication, which decreases the COF of the coating. As a result, the AlTiN coating prepared by CAIP has excellent antifriction and wear resistance properties.
2. The average COFs of the AlTiN coating under loads of 5, 7, and 9 N are 0.6495, 0.5897, and 0.3898, respectively, which decreases with increasing loads, showing that the

AlTiN coating can be applied for surface modification of cutting tools under heavy loads at high temperature.

- The contents of Al, Ti, and N elements on the wear track were decreased after wear at 800°C and the N element was fully released, whereas the content of O element on the wear track increased greatly, showing that the wear mechanism of AlTiN coating was primarily oxidation wear and abrasive wear, accompanied by fatigue wear and adhesive wear.

## Funding

Financial support for this research by the Jiangsu Province Science and Technology Support Program (Industry) (BE2014818) is gratefully acknowledged.

## References

- Zhang, H. P., Wang, S. R., Guo, P. Q., and Wang, M. (2013), "Microstructure and Wear Properties Analysis of TiAlN Film Deposited on Cam Profile Using Ion Sputtering," *Tribology Transactions*, **56**(6), pp 968–976.
- Kong, D. J. and Fu, G. Z. (2015), "Nanoindentation Analysis of TiN, TiAlN and TiAlSiN Coatings Prepared by Cathode Ion Plating," *Science China Technological Sciences*, **58**(1), pp 1360–1368.
- Tian, B., Wen, Y., Fu, Z. Q., Gu, Y. H., Wang, C. B., and Liu, J. J. (2014), "Microstructure and Tribological Properties of W-implanted PVD TiN Coatings on 316L Stainless Steel," *Vacuum*, **99**, pp 68–75.
- Chang, Y. Y. and Wang, D. Y. (2007), "Characterization of Nanocrystalline AlTiN Coatings Synthesized by a Cathodic-Arc Deposition Process," *Surface and Coatings Technology*, **201**(15), pp 6699–6701.
- Jílek, M. J., Jílek, M., Mendez, M. F., Mayrhofer, P. H., and Veprek, S. (2014), "High-Rate Deposition of AlTiN and Related Coatings with Dense Morphology by Central Cylindrical Direct Current Magnetron Sputtering," *Thin Solid Films*, **556**, pp 361–368.
- Halil, Ç., Peter, P., and Srecko, P. (2014), "Monitoring of Wear Characteristics of TiN and TiAlN Coatings at Long Sliding Distances," *Tribology Transactions*, **57**(3), pp 496–502.
- Kong, D. J. and Guo, H. Y. (2015), "Analysis of Structures and Bonding Strength of AlTiN Coatings by Cathodic Ion Plating," *Applied Physics A: Materials Science & Processing*, **119**, pp 309–316.
- Wang, X., Parick, Y. K., David, S., and Dave K. (2013), "Friction Coefficient and Sliding Wear of AlTiN Coating under Various Lubrication Conditions," *Wear*, **304**(1–2), pp 67–76.
- Kong, D. J. and Guo, H. Y. (2015), "Friction–Wear Behaviors of Cathodic Arc Ion Plating AlTiN Coatings at High Temperatures," *Tribology International*, **88**, pp 31–39.
- Xie, Z. W., Wang, L. P., Wang, X. F., Yan, J. C., Huang, L., and Lu, Y. (2011), "High Temperature Oxidization Resistance and Wear Properties of TiAlN Coatings Deposited by MPIIID," *Tribology*, **31**(2), pp 175–180.
- Radhika, R., Kumar, N., Pandian, R., Dash, S., Ravindran, T. R., Arivuoli, D., and Tyagi, A. K. (2013), "Tribological Properties and Deformation Mechanism of TiAlN Coating Sliding with Various Counterbodies," *Tribology International*, **66**, pp 143–149.
- Fu, C. S. (1993), *Principle of non-ferrous metallurgy*, Metallurgical Industry Press: Beijing.
- Yucel, B. (2013), "Sliding Wear of CrN, AlCrN and AlTiN Coated AISI H13 Hot Work Tool Steels in Aluminium Extrusion," *Tribology International*, **57**, pp 101–106.
- Chen, L., Yang, B., Xu Y. X., Pei, F., Zhou, L. C., and Du, Y. (2014), "Improved Thermal Stability and Oxidation Resistance of Al-Ti-N Coating by Si Addition," *Thin Solid Films*, **556**, pp 369–375.
- Soner, S. and Şengül, D. (2014), "Multipass Sliding Wear Behavior of TiAlN Coatings Using a Spherical Indenter: Effect of Coating Parameters and Duplex Treatment," *Tribology Transactions*, **57**(2), pp 242–255.
- Biksa, A., Yamamoto, K., Dosbaeva, G., Veldhuis, S. C., Fox-Rabinovich, G. S., Elfizy, A., Wagg, T., and Shuster, L. S. (2010), "Wear Behavior of Adaptive Nano-Multilayered AlTiN/Me<sub>x</sub>N PVD Coatings during Machining of Aerospace Alloys," *Tribology International*, **43**(8), pp 1491–1499.